ISSN 1674-1056
http://cpb.iphy.ac.cn
http://iopscience.iop.org/cpb
中国物理 B
Chinese Physics
中国物理
Chinese Physics B

Distinct edge states and optical conductivities in the zigzag and armchair silicene nanoribbons under exchange and electric fields

Jianfei Zou(邹剑飞), Jing Kang(康静)
Citation: Chin. Phys. B . 2018, 27(3): 037301. **doi:** 10.1088/1674-1056/27/3/037301

Journal homepage: http://cpb.iphy.ac.cn; http://iopscience.iop.org/cpb

What follows is a list of articles you may be interested in

Band structure and edge states of star-like zigzag graphene nanoribbons

Hong Liu(刘红)
Chin. Phys. B . 2017, 26(11): 117301. **doi:** 10.1088/1674-1056/26/11/117301

Quantum transport through a Z-shaped silicene nanoribbon

A Ahmadi Fouladi
Chin. Phys. B . 2017, 26(4): 047304. **doi:** 10.1088/1674-1056/26/4/047304

Two-dimensional topological insulators with large bulk energy gap

Z Q Yang(杨中强), Jin-Feng Jia(贾金锋), Dong Qian(钱冬)
Chin. Phys. B . 2016, 25(11): 117312. **doi:** 10.1088/1674-1056/25/11/117312

Effect of disorders on topological phases inone-dimensional optical superlattices

Zhizhou Wang(王志宙), Yidong Wu(吴一东), Huijing Du(杜会静), Xili Jing(井西利)
Chin. Phys. B . 2016, 25(7): 077303. **doi:** 10.1088/1674-1056/25/7/077303

Topological edge states and electronic structures of a 2D topological insulator: Single-bilayer Bi (111)

Gao Chun-Lei, Qian Dong, Liu Can-Hua, Jia Jin-Feng, Liu Feng
Chin. Phys. B . 2013, 22(6): 067304. **doi:** 10.1088/1674-1056/22/6/067304

Distinct edge states and optical conductivities in the zigzag and armchair silicene nanoribbons under exchange and electric fields*

Jianfei Zou(邹剑飞)† and Jing Kang(康静)

College of Science, Hohai University, Nanjing 210098, *China*

(Received 12 September 2017; revised manuscript received 22 December 2017; published online 11 February 2018)

Based on the tight binding model, we investigate the low energy bandstructures, edge states, and optical absorptions for the silicene nanoribbons (SiNRs) with different terminations under an in-plane exchange field and/or a perpendicular electric field. We find that the zigzag SiNRs are gapped by the exchange field, but they could reenter the metallic state after the application of the electric field. Contrarily, a certain kind of armchair SiNRs remain gapless even if a weak exchange field is present. Furthermore, the combination of the exchange and electric fields could effectively modulate the penetration length and the components of the edge states in the SiNRs. The corresponding optical conductivities for the SiNRs are also calculated, which show remarkable dependence on the edge types of the SiNRs and the two external fields.

Keywords: silicene nanoribbon, edge state, optical conductivity, exchange field

PACS: 73.20.At, 78.67.–n, 81.05.ue **DOI:** 10.1088/1674-1056/27/3/037301

1. Introduction

Silicene is a two-dimensional allotrope of silicon, whose atoms are packed in a honeycomb lattice similar to that of graphene. It has motivated many studies since its successful synthesis and characterization in experiments.[1–3] Distinct from graphene, the two sublattice planes in silicene are separated by a distance of 0.46 Å due to the buckled structure, which results in an observable spin-orbit gap.[4] As a result, its Dirac cones at K valleys in the Brillouin zone are gapped by the spin–orbit interaction (SOI), which indicates the topologically nontrivial properties of silicene. It has been predicted that silicene exhibits some peculiar phenomena, such as the quantum spin Hall effect,[5] quantum anomalous Hall effect,[6,7] and spin-valley coupled optical responses.[8,9] The external fields, such as the perpendicular electric field and out of plane exchange field, could drive a rich variety of phase transitions in silicene.[6,10] In addition, the combination of the intrinsic and Rashba SOIs could enhance the optical spin current injection in a silicene sheet.[11]

By cutting a single layer silicene sheet, one obtains quasi-one dimensional silicene nanoribbons (SiNRs), which have also been synthesized in experiments.[12–14] Similar to their cousins graphene nanoribbons, SiNRs possess abundant physical properties due to the quantum confinement effect.[15] The electronic structures of the SiNRs could be engineered by controlling the electric field,[16,17] strain,[18,19] and doping,[20] which makes the SiNRs have promising application prospect in the silicon-based spintronics and optoelectronics. What is more, the SiNRs inherit the nontrivial topology of the silicene. It has been found that the topological edge states are fundamentally different between the armchair and zigzag edges. Cano-Cortés and her collaborators found that the Fermi velocity of the edge states at the zigzag terminators is linear with the strength of the SOI, whereas that at the armchair terminators is independent of the SOI.[21] Ezawa and Nagaosa found that the penetration depth of the edge states for the armchair SiNRs (ASiNRs) is inversely proportional to the SOI, but that for the zigzag SiNRs (ZSiNRs) remains as short as the lattice constant.[22] Besides, some researches on the optical responses of the SiNRs have been reported. Specifically, Bao and his co-workers studied the transition rule and the ultraviolet optical response in the ASiNRs.[23,24] Shyu investigated the optical properties of the ASiNRs modulated by a transverse electric field and those of ZSiNRs in a perpendicular magnetic field.[25,26] Here we ask such questions, how do the electric and exchange fields affect the energy bands and the edge states of the SiNRs? Could we modulate the unique edge states conveniently by controlling the external fields and identify them by the optical measurement?

To answer these questions, in this paper, we investigate the bandstructures, edge states, and optical absorptions of the zigzag and armchair SiNRs under the influence of an in-plane exchange field and/or a perpendicular electric field. It is found that the properties of the edge states remarkably depend on the edge types of the SiNRs and the two external fields. The remainder of the work is arranged as follows. In Section 2, the theoretical model for the SiNRs is described. In Section 3, the low energy bandstructures, as well as the distributions of the edge states, are demonstrated. In Section 4, the optical conductivities of the SiNRs are calculated. Finally, a brief conclusion is given in Section 5.

*Project supported by the National Natural Science Foundation of China (Grant Nos. 11347127, 61404044, and 11347111).

†Corresponding author. E-mail: zoujianfei@hhu.edu.cn

© 2018 Chinese Physical Society and IOP Publishing Ltd

2. Model

Let us consider a monolayer zigzag or armchair SiNR with its two boundaries extending along the longitudinal direction, as illustrated in Fig. 1. A pristine SiNR could be mimicked by the following tight binding Hamiltonian:[27]

$$H_0 = -t_0 \sum_{\langle ij\rangle\alpha} c^{\dagger}_{i,\alpha} c_{j,\alpha} + \frac{\mathrm{i}\lambda_{\mathrm{SO}}}{3\sqrt{3}} \sum_{\langle\langle ij\rangle\rangle\alpha\beta} v_{ij} c^{\dagger}_{i,\alpha} s_{z,\alpha\beta} c_{j,\beta}, \quad (1)$$

where $c^{\dagger}_{i,\alpha}$ and $c_{i,\alpha}$ denote the creation and annihilation operators of electron at lattice site i with spin α, respectively. The summations of $\langle i,j\rangle$ and $\langle\langle i,j\rangle\rangle$ go through all of the pairs of the nearest and the next-nearest neighbor sites, respectively. $t_0 = 1.6$ eV is the nearest-neighbor transfer integral. The first term in the Hamiltonian above describes the standard nearest-neighbor hopping. (s_x, s_y, s_z) represents the vector of the Pauli matrix for the electron spin and the factor $v_{ij} = 1$ (-1) indicates the anticlockwise (clockwise) next-nearest neighbor hopping about the $+z$ axis. The second term represents the intrinsic SOI term. In silicene, the parameter for the SOI λ_{SO} is 3.9 meV. Here the intrinsic Rashba SOI in silicene is ignored due to its very small value about 0.7 meV.[28] For the sake of simplicity, we do not consider the modification of the transfer energy at the boundaries either.

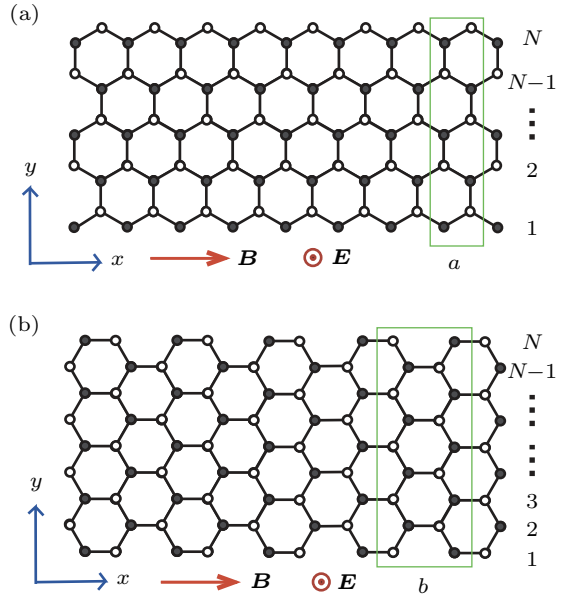


Fig. 1. (color online) Structures of SiNRs with (a) zigzag and (b) armchair edges. Here the number of the longitudinal diatomic chains of the SiNRs $N = 6$ in panel (a) and $N = 9$ in panel (b). The rectangle denotes a unit cell including $2N$ atoms. $a = 3.86$ Å is the lattice constant of the zigzag SiNRs and $b = \sqrt{3}a = 6.69$ Å is that of the armchair SiNRs. A perpendicular electric field $\boldsymbol{E}$ and an in-plane magnetic field $\boldsymbol{B}$ are applied.

As the SiNR is subjected to a perpendicular electric field, a staggered sublattice potential emerges due to the buckled structure of silicene. Besides, an in-plane exchange field could also be introduced in the SiNR. They are summarized as an additional term to the previous Hamiltonian, which is written as

$$H_1 = \lambda_{\mathrm{V}} \sum_{i\alpha} \xi_i c^{\dagger}_{i,\alpha} c_{i,\alpha} + \lambda_{\mathrm{m}} \sum_{i\alpha\beta} c^{\dagger}_{i,\alpha} s_{x,\alpha\beta} c_{i,\beta}, \quad (2)$$

where $\xi_i = \pm 1$ with i denoting the A (B) site and the Greek letters α and β label the spin polarization $\uparrow$ or $\downarrow$. The first term represents the staggered sublattice potential with its strength λ_{V} proportional to the electric field. And the second term describes the exchange (Zeeman) term with the exchange energy (Zeeman splitting) λ_{m}. We point out that the later could be induced in the SiNR via the proximity effect of a ferromagnet substrate[6,29,30] or by applying a magnetic field parallel to the sample. We will find that the effect of the in-plane exchange field on the SiNRs is quite different from that of the out-of-plane exchange field. Here the in-plane exchange field is set along the x direction (its direction does not affect the results of this paper). Consequently, the total Hamiltonian for the SiNR under the two external fields is written as $H = H_0 + H_1$.

For the SiNRs translate invariantly along the longitudinal direction, Fourier transformation can be performed on the x component of the total Hamiltonian H. Then one obtains a new Hamiltonian $\mathcal{H}(k_x)$ with k_x being the Bloch wavevetor in the x direction, which is a $4N \times 4N$ Hermitian matrix including the contributions from the orbitals and spins. By diagonalizing the Hermitian matrix, we can acquire the energy spectra $E_{n_{\mathrm{c(v)}}}(k_x)$ and the corresponding wave functions $|n_{\mathrm{c(v)}}, k_x\rangle$, in which $n_{\mathrm{c(v)}}$ denotes the index of the conduction (valence) subbands arranged in the order of the energy difference between the subband and the Fermi level.

3. Bandstructures and edge states

Next, we present some numerical results of the low energy bandstructures and edge states for the SiNRs with different terminations. Hereafter we refer to the ZSiNR with N zigzag chains as N-ZSiNR and the SiNR with N dimer chains as N-ASiNR. To show the effects of the SOI and the external fields clearly, we fix the parameter of the SOI $\lambda_{\mathrm{SO}} = 0.1t_0$ throughout this work.

3.1. Zigzag nanoribbons

Figure 2 exhibits the electronic structures at low energy for a 30-ZSiNR without and with the in-plane exchange field and/or the perpendicular electric field. The width of the nanoribbon is about 10.0 nm ($W = \sqrt{3}Na/2$). When both of the exchange and electric fields are absent, as shown in Fig. 2(a), one sees that the energy spectrum possesses the spin degeneracy, the electron–hole symmetry, and the symmetry about the wavevector $k_x = \pi/a$. Furthermore, the highest valance subband ($n_{\mathrm{v}} = 1$) and the lowest conduction subband ($n_{\mathrm{c}} = 1$) cross at $k_x = \pi/a$, resulting a linear dispersion

near zero energy. It has been confirmed that the gapless states are spin–momentum locked, which characterizes the quantum spin Hall state.[31] When an exchange field is taken into the nanoribbon, each of the previous bulk subbands with spin degeneracy splits into two subbands, as illustrated in Fig. 2(b). However, the edge states still keep the spin degeneracy, and a gap about $2\lambda_{\rm m} = 0.06t_0$ is opened by the in-plane exchange field. Incidentally, we emphasize that the out-of-plane exchange field could not open a gap but raise the spin-up subbands and lower the spin-down subbands.

When the perpendicular electric field is applied to the 30-ZSiNR, the ZSiNR remains gapless, although the spin degeneracy of all subbands is broken, as shown in Fig. 2(c). In particular, the energy level of the edge states localized at one edge shifts upwards by $\lambda_{\rm V} = 0.05t_0$, while that of the others localized at the opposite edge shifts downwards by $0.05t_0$. Applying both of the external fields in the system, we show the bandstructures of ZSiNR in Fig. 2(d). It is found that the edge states at both of the two edges are gaped by about $0.06t_0$, meanwhile their corresponding subbands shift upwards and downwards, respectively. In other words, the electric field drives the semiconducting ZSiNR with an in-plane exchange field into the metallic state.

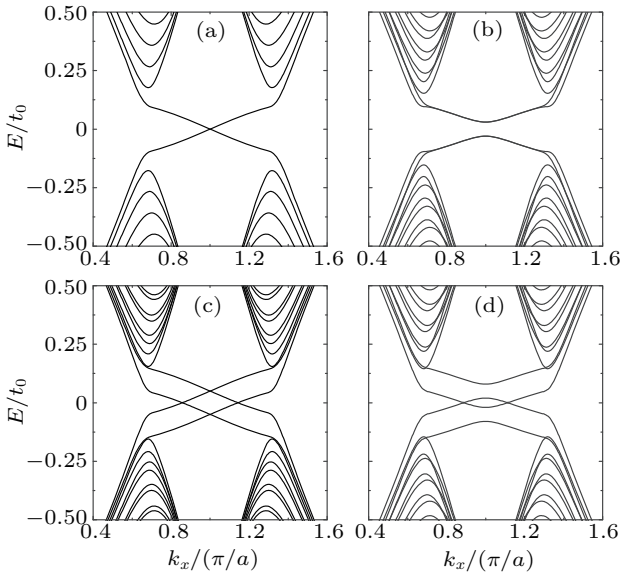


Fig. 2. Low energy electronic structures of 30-ZSiNR (a) without external fields, (b) with the in-plane exchange field, (c) with the perpendicular electric field, and (d) with both of the exchange and electric fields. The parameters are set to be $\lambda_{\rm m} = 0.03t_0$ and $\lambda_{\rm V} = 0.05t_0$.

In order to demonstrate the edge states clearly, we plot the distribution of the probability density of the edge states in the 30-ZSiNR under the exchange field, i.e., the squared modulus of the wavefunction for the edge states close to the Fermi level, as shown in Fig. 3. When the electric field is absent, it is found that the edge states are almost localized at the sites of the two boundaries, as shown in Fig. 3(a). We also find that the exchange field rarely changes the penetration length of the localized edge states. However, it mixes the components of spin up and down for the edge states. When the electric field is applied, the penetration of the edge states into the bulk becomes obvious. But the mixture of the different spin components for the edge states is suppressed, as shown in Fig. 3(b).

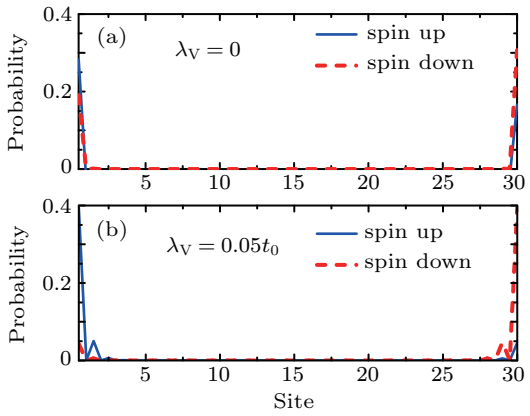


Fig. 3. (color online) Probability distributions of the edge states near the Fermi level in the 30-ZSiNR with the exchange field $\lambda_{\rm m} = 0.03t_0$ (a) but without and (b) under the electric field. Here the electrons in these edge states propagate along the $+x$ direction.

As for the wider ZSiNRs, the results of the bandstructures and the edge states are similar to those for the 30-ZSiNR. In fact, if we study an half-infinite silicene with zigzag terminations in the x direction, a phenomenological effective Hamiltonian for the edge states could be obtained: $H_{\rm e} = \hbar v_{\rm F} k_x s_z + \lambda_{\rm m} s_x \pm \lambda_{\rm V}$, where $v_{\rm F} = \sqrt{3}\lambda_{\rm SO} a/2$ is the Fermi velocity for the edge states. Then the dispersions for the edge states are obtained as $E_{\rm e} = \pm\sqrt{(\hbar v_{\rm F} k_x)^2 + \lambda_{\rm m}^2} \pm \lambda_{\rm V}$ and the gap $\Delta E_{\rm e} = 2\lambda_{\rm m}$. These analytical dispersions fit the edge states near zero energy in Fig. 2 very well.

3.2. Armchair nanoribbons

Now let us consider the case of the armchair nanoribbons. It is well known that the graphene nanoribbons with armchair edges can be classified into two categories: one type with $N = 3l$, $3l+1$ (l is an integer) is semiconducting, whereas the other with $N = 3l+2$ is semimetallic. The first-principle calculations demonstrate that this classification is also applicable for the ASiNRs with buckled structure and weak SOI.[16] Figure 4 displays the low energy electronic structures for a semiconducting 30-ASiNR with or without the exchange and/or electric fields. Its width is 5.79 nm ($W = Na/2$). It is found that the in-plane exchange field eliminates the spin degeneracy of all subbands and decreases the gap from $0.063t_0$ in Fig. 4(a) to $0.035t_0$ in Fig. 4(b). In contrary, the staggered sublattice potential maintains the spin degeneracy and increases the gap up to $0.086t_0$, as shown in Fig. 4(c). The competition of the two external fields gives rise to the spin split subbands and a gap about $0.058t_0$ in Fig. 4(b). As the width of the semiconducting

ASiNRs increases, all of the gaps of the ASiNRs in these different cases decrease due to a weaker hybridization between the edge states localized at the opposite edges.

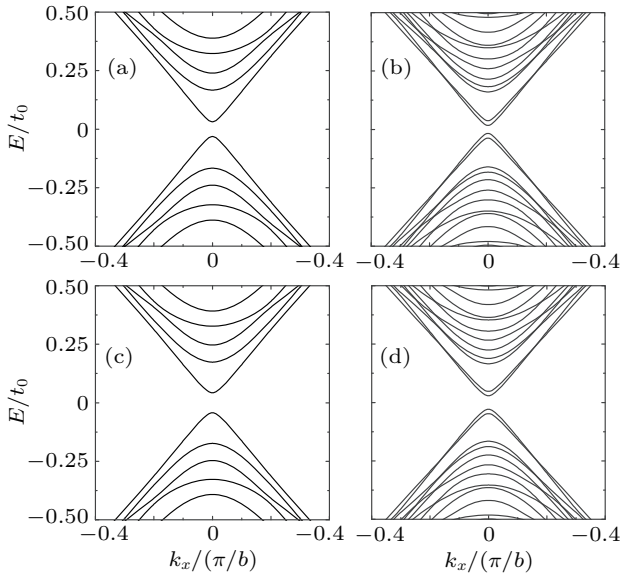


Fig. 4. Low energy electronic structures of 30-ASiNR (a) without external fields, (b) with the exchange field, (c) with the electric field, and (d) with both of the two external fields. The parameters are the same as those in Fig. 2.

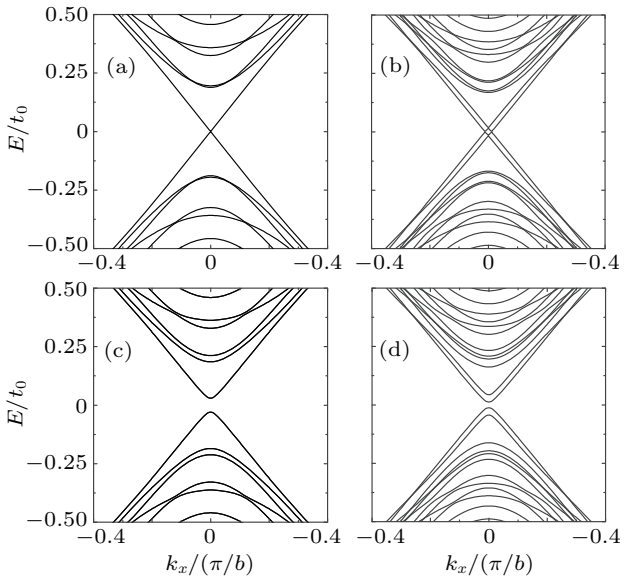


Fig. 5. Low energy electronic structures of 32-ASiNR (a) without external fields, (b) with the exchange field, (c) with the electric field, and (d) with both of the two external fields. The parameters are the same as those in Fig. 2.

In Fig. 5, we show the band structures for a semimetallic 32-ASiNR. Its width is 6.18 nm. When the exchange field is induced in the ASiNR, one finds that the 32-ASiNR is still gapless, although the degeneracy of all subbands including that of the edge states is eliminated, as shown in Fig. 5(b). Actually, there is an extremely tiny gap about $0.003t_0$. We can demonstrate that the ignorable gap approaches to zero as the width of the ASiNR increases, while the 32-ASiNR under the electric field opens a gap about $0.060t_0$ (see Fig. 5(c)). When both of the two external fields are taken into account, the spin subbands split and a narrower gap about $0.024t_0$ is obtained, as illustrated in Fig. 5(d). Similar to the semiconducting ASiNRs, the semimetallic ASiNRs in the different fields become wider, the corresponding gaps for the edge states become narrower and eventually faint. These are fundamentally distinct from the results for the ZSiNRs.

We plot the distribution of the probability density of the edge states for a semiconducting 60-ASiNR with an exchange field in Fig. 6. One sees that the edge states localized at the two edges remarkably oscillate with considerable damping, whose penetration depth is far larger than that in the ZSiNRs. Actually, the penetration depth for the ASiNRs is approximately inversely proportional to that for the ZSiNRs.[22] It is found that the penetration depth is increased by the electric field but nearly unaffected by the exchange field, that is alike to the results of the ZSiNRs. However, the edge state at one edge of the ASiNR is nearly fully spin-polarized, which differs from that in the ZSiNRs under an exchange field. We also find that there is no obvious difference of the edge state distributions between the semiconducting and semimetallic ASiNRs.

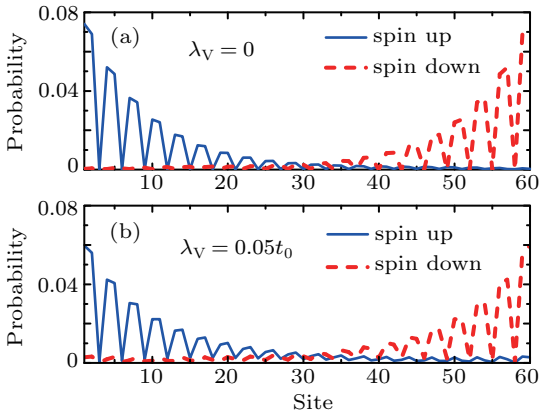


Fig. 6. (color online) Probability distributions of the edge states near the Fermi level in the 60-ASiNR with the exchange field $\lambda_m = 0.03t_0$ (a) but without and (b) under the electric field. Here the electrons in these edge states propagate along the $+x$ direction.

We have found that the in-plane exchange field could not induce a considerable gap for the edge states in the semiconducting and semimetallic ASiNRs, which completely differs from the result for the ZSiNRs. Indeed, when the ASiNR becomes wide enough, the hybridization of the edge states could be ignorable, such that all of the edge states in the sufficiently wide ASiNR stay gapless even if a weak exchange field and/or a weak electric field is applied. Furthermore, our numerical calculations show that the Fermi velocity of the gapless edge states for the wide ASiNRs is decreased by the exchange field and is almost independent of the electric field.

It should be emphasized that the band structures and the edge states are obtained under the condition that both of the staggered potential and the exchange field are smaller than the

intrinsic SOI. In this case, the gap of the bulk states is dominated by the intrinsic SOI. That is to say, the SiNRs are in the topological insulator state. If the staggered potential is larger than the intrinsic SOI, the SiNRs will become band insulators. As a result, there is no topologically protected edge state in the SiNRs. On the other hand, if the exchange field is large enough, the band structures and the edge states will change completely.

4. Optical conductivities

In experiments, the distinct electronic structures and edge states for the SiNRs with different edges under the external fields can be characterized by measuring the optical absorption spectra. In the following, let us consider a beam of monochromatic light irradiating on the SiNRs, whose polarization is linear in the x direction. In the frame of the linear response theory, the real part of the optical conductivity can be written as

$$\sigma(\omega) = \frac{\pi e^2}{S\omega} \sum_{n,n',k_x} \left|\langle n', k_x|\hat{v}_x|n, k_x\rangle\right|^2 [f(E_{n',k_x}) - f(E_{n,k_x})] \times \delta(E_{n',k_x} - E_{n,k_x} - \hbar\omega), \quad (3)$$

where ω is the light frequency, S is the area of the nanoribbon, and e is the charge of electron. $\langle n', k_x|\hat{v}_x|n, k_x\rangle$ is a matrix element for the optical transition between states $|n, k_x\rangle$ and $|n', k_x\rangle$. $\hat{v}_x = \hbar^{-1}\partial\mathcal{H}/\partial k_x$ is the velocity operator in the x direction. In the limit of low temperature, it can be assumed that the Fermi–Dirac distribution function $f(E_{n,k_x}) = 1$ for $E_{n,k_x} < E_F$ and $f(E_{n,k_x}) = 0$ for $E_{n,k_x} > E_F$, where E_F is the Fermi energy. In this work, we consider the undoped SiNRs at low temperature so that $E_F = 0$. In the following numerical calculations, the Dirac delta function in Eq. (3) is replaced by a Lorenzian function with a broadening width $\eta = 0.003t_0$.

4.1. Zigzag nanoribbons

Figure 7 demonstrates the optical conductivities for the 30-ZSiNR in different fields. For the pristine ZSiNR, the first absorption peak A_1 at $\hbar\omega = 0.21t_0$ is generated from the electron transition between the edge states, as shown in Fig. 7(a). The second main peak A_2 at $\hbar\omega = 0.28t_0$ is contributed by the transitions $n_v \to n_c : 1(2) \to 2(1)$. The other peaks are dominated by the transitions between the bulk states. After applying an in-plane exchange field in the ZSiNR, a richer optical spectrum emerges, which is attributed to the spin splitting of the subbands. In particular, the first two subpeaks B_1 and B_2 at $\hbar\omega = 0.06t_0, 0.20t_0$ are contributed by the transitions between the edge states at the vicinities of the center of the Brillouin zone and K points, respectively. The first peak B_1 at $\hbar\omega = 0.06t_0$ indicates the gap of the edge states opened by the in-plane exchange field. When the perpendicular electric field is introduced in the 30-ZSiNR without the exchange field, a weak peak C_1 at $\hbar\omega = 0.10t_0$ appears, which is attributed to the optical transition $n_v \to n_c : 1 \to 1$, while the second peak C_2 at $\hbar\omega = 0.21t_0$ comes from the transitions between the edge and bulk states, as shown in Fig. 7(b). When both of the exchange and electric fields are present, the previous peaks shift, and there are no additional peaks. Particularly, a possible peak at $\hbar\omega = 0.06t_0$ due to the gap of the edge states is absent, this is because both of the two energy states near $k_x = \pi/a$ for one edge are occupied while those for the opposite edge are unoccupied, as shown in Fig. 2(d). In a word, for the ZSiNRs, both of the two external fields could bring about some featured absorption peaks due to the splitting of the subbands.

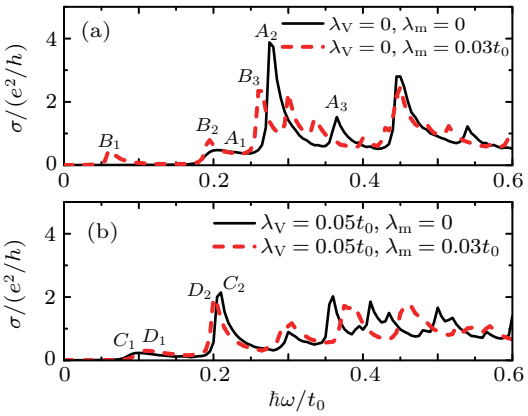


Fig. 7. (color online) Optical conductivities of the 30-ZSiNR in different fields.

4.2. Armchair nanoribbons

In Fig. 8, we plot the optical conductivities versus the light frequency for the semiconducting 30-ASiNR with and without the external fields. In Fig. 8(a), one can see three absorption peaks in the solid line due to the direct interband transitions: $\Delta n = |n_c - n_v| = 0$, which are valid near the Dirac points. This selection rule is the same as that in the pristine armchair graphene nanoribbon,[25,32] which quite differs from that for the ZSiNRs. In particular, the first absorption peak A_1 at $\hbar\omega = 0.065t_0$ is the signature of the energy gap. After considering the in-plane exchange field, additional absorption peaks emerge because the transition rule is modified. One finds that two subpeaks, labeled as B_2 at $\hbar\omega = 0.18t_0$ and B_3 at $\hbar\omega = 0.22t_0$, come from the electron transitions $\Delta n = 2$ ($n_v \to n_c : 1(3) \to 3(1)$) and $\Delta n = 2, 4$ ($n_v \to n_c : 2(4) \to 4(2), 1(5) \to 5(1)$), respectively. Furthermore, one should note that the frequency $\hbar\omega = 0.055t_0$ for the threshold peak B_1, which is due to the transition between the edge states $\Delta n = 1$ ($n_v \to n_c : 1(2) \to 2(1)$), is larger than the energy gap $\Delta E_g = 0.035t_0$ for the 30-ASiNR in the exchange field. When the electric field is taken into consideration in the ASiNR, the selection rule for the optical absorption remains unchanged, such that the previous absorption peaks still exist but shift a little as shown in Fig. 8(b).

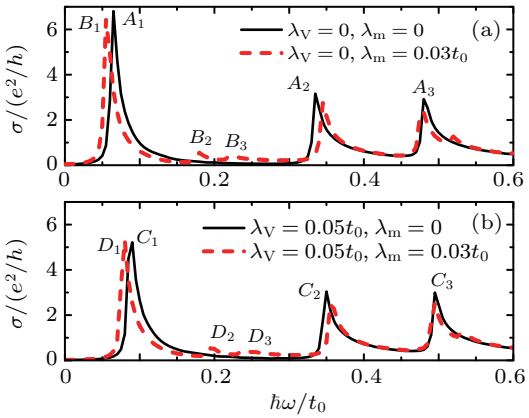


Fig. 8. (color online) Spectra of the optical conductivity for the 30-ASiNR (a) without and (b) under the perpendicular electric field.

We also present the spectra of the optical conductivities for the semimetallic 32-ASiNR in different fields, as shown in Fig. 9. In Fig. 9(a), there is a very high peak A_1 at the limit of the low frequency due to the existence of the extremely tiny gap in the ASiNR. One can also find two overlapped peaks A_2 and A_3 near $\hbar\omega = 0.39t_0$, which are attributed to the transitions $n_v \to n_c : 2(3) \to 2(3)$. When the in-plane exchange field is taken into account in the ASiNR, the impractical peak near the zero frequency is absent because of a little shift of the Dirac points away from the Fermi level (see Fig. 5(b)). However, the other previous peaks are almost unaffected by the exchange field. Meanwhile, an unclear broad subpeak or plateau B_1 near $\hbar\omega = 0.25t_0$ emerges, which indicates the feeble transitions between the edge and bulk states. When the electric field is considered, the absorption spectra of the 32-ASiNR are similar to those of the 30-ASiNR, as illustrated in Fig. 9(b). In summary, for the ASiNRs, the in-plane exchange field could give rise to some new absorption peaks contributed by the transitions between the edge and bulk states, whereas the perpendicular electric field only brings about the shift of the absorption peaks.

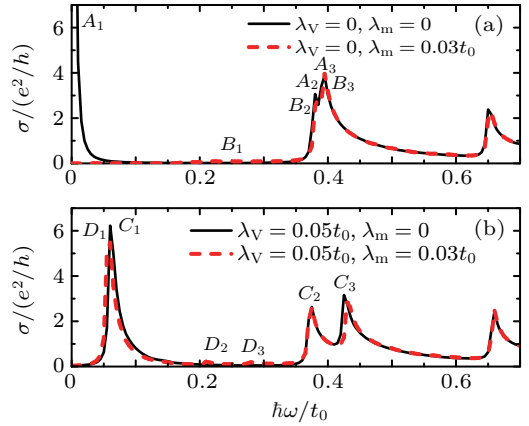


Fig. 9. (color online) Spectra of the optical conductivity for the 32-ASiNR in different cases.

Based on the above results, it could be inferred that the difference of the optical transitions between the armchair- and zigzag-edge silicene nanoribbons originates from their geometrical structures, especially the edge structures, and the symmetry of the energy bands. By the way, our further calculations show that there is no obvious difference between the optical transitions in the odd- and even-ZSiNRs. However, we could expect that the spin transport and thermopower in the ZSiNRs should display the even–odd behavior.[33,34] In addition, it is noted that more complicated optical transitions in the ASiNRs, for instance $n_v \to n_c$: odd/even $\to$ even/odd, could emerge if we consider a larger range of frequency and adopt different calculation methods.[23,24,35]

5. Conclusion

We have investigated the low energy electronic structures, edge states, and optical absorptions for the zigzag and armchair SiNRs under an in-plane exchange field and/or a perpendicular electric field. We find that the gap and the edge states in the SiNRs could be engineered by the combination of the two external fields. Particularly, the in-plane exchange field could drive the ZSiNRs into the insulating phase, whereas the perpendicular electric field could make them metallic again. On the contrary, the exchange field keeps the metallic ASiNRs in the metallic state, but the electric field leads them into the insulating phase. Furthermore, it is inferred that the gapless edge states in the wide ASiNRs survive even if both of the two weak external fields are applied. It is also found that the penetration length and the components of the edge states could be modified by the electric and exchange fields, respectively. We can also demonstrate that the fundamental distinct edge states in the SiNRs with different edges under the external fields could be detected by the optical absorptions. These findings indicate that SiNRs are promising materials for designing the silicon-based spintronics nanodevices.

References

[1] Vogt P, Padova P D, Quaresima C, Avila J, Frantzeskakis E, Asensio M C, Resta A, Ealet B and Lay G L 2012 *Phys. Rev. Lett.* **108** 155501
[2] Fleurence A, Friedlein R, Ozaki T, Kawai H, Wang Y and Yamada-Takamura Y 2012 *Phys. Rev. Lett.* **108** 245501
[3] Meng L, Wang Y, Zhang L, Du S, Wu R, Li L, Zhang Y, Li G, Zhou H, Hofer W A and Gao H J 2013 *Nano Lett.* **13** 685
[4] Ni Z, Liu Q, Tang K, Zheng J, Zhou J, Qin R, Gao Z, Yu D and Lu J 2012 *Nano Lett.* **12** 113
[5] Liu C C, Feng W and Yao Y 2011 *Phys. Rev. Lett.* **107** 076802
[6] Ezawa M 2012 *Phys. Rev. Lett.* **109** 055502
[7] Pan H, Li Z, Liu C C, Zhu G, Qiao Z and Yao Y 2014 *Phys. Rev. Lett.* **112** 106802
[8] Ezawa M 2012 *Phys. Rev. B* **86** 161407
[9] Stille L, Tabert C J and Nicol E J 2012 *Phys. Rev. B* **86** 195405
[10] Wang S K, Tian H Y, Yang Y H and Wang J 2014 *Chin. Phys. B* **23** 017203
[11] Zou J, Tang C and Zhang A 2017 *Phys. Lett. A* **381** 1197
[12] Léandri C, Oughaddou H, Aufray B, Gay J M, Le Lay G, Ranguis A and Garreau Y 2007 *Surf. Sci.* **601** 262
[13] Aufray B, Kara A, Vizzini S, Oughaddou H, Léandri C, Ealet B and Le Lay G 2010 *Appl. Phys. Lett.* **96** 183102

[14] Padova P D, Quaresima C, Ottaviani C, Sheverdyaeva P M, Moras P, Carbone C, Topwal D, Olivieri B, Kara A, Oughaddou H, Aufray B and Lay G L 2010 *Appl. Phys. Lett.* **96** 261905
[15] Cahangirov S, Topsakal M, Aktürk E, Şahin H and Ciraci S 2009 *Phys. Rev. Lett.* **102** 236804
[16] Ding Y and Ni J 2009 *Appl. Phys. Lett.* **95** 083115
[17] Liang Y, Wang V, Mizuseki H and Kawazoe Y 2012 *J. Phys.: Condens. Matter* **24** 455302
[18] Lian C, Yang Z and Ni J 2013 *Chem. Phys. Lett.* **561** 77
[19] Mahmoudi M, Ahangari Z and Fathipour M 2016 *Chin. Phys. B* **25** 018501
[20] Ma L, Zhang J M, Xu K W and Ji V 2013 *Physica B* **425** 66
[21] Cano-Cortés L, Ortix C and van den Brink J 2013 *Phys. Rev. Lett.* **111** 146801
[22] Ezawa M and Nagaosa N 2013 *Phys. Rev. B* **88** 121401
[23] Bao H, Liao W, Guo J, Yang X, Zhao H and Zhou G 2015 *J. Phys. D: Appl. Phys.* **48** 455306
[24] Liao W, Bao H, Zhang X, Yang X, Zhang Z and Zhao H 2016 *Appl. Phys. A* **122** 464
[25] Shyu F L 2017 *Physica E* **85** 117
[26] Shyu F L 2017 *Physica E* **87** 178
[27] Kane C L and Mele E J 2005 *Phys. Rev. Lett.* **95** 146802
[28] Liu C C, Jiang H and Yao Y 2011 *Phys. Rev. B* **84** 195430
[29] Zou J, Jin G and Ma Y Q 2009 *J. Phys.: Condens. Matter* **21** 126001
[30] Wei P, Lee S, Lemaitre F, Pinel L, Cutaia D, Cha W, Katmis F, Zhu Y, Heiman D, Hone J, Moodera J S and Chen C T 2016 *Nat. Mater.* **15** 711
[31] Kane C L and Mele E J 2005 *Phys. Rev. Lett.* **95** 226801
[32] Sasaki K I, Kato K, Tokura Y, Oguri K and Sogawa T 2011 *Phys. Rev. B* **84** 085458
[33] Tian H Y and Wang J 2012 *Chin. Phys. B* **21** 017203
[34] Zhou B, Zhou B, Chen X, Liao W and Zhou G 2015 *J. Phys.: Condens. Matter* **27** 465301
[35] Liao W, Zhou G and Xi F 2008 *J. Appl. Phys.* **104** 126105